REPORT DOCUMENTATION PAGE

Form Approved OMB NO. 0704-0188

1. REPORT DATE (DD-MM-YYYY)	2. REPORT TYPE	3. DATES COVERED (From - To)
18-08-2009	Final Report	18-Jul-2005 - 17-May-2009

4. TITLE AND SUBTITLE
On-Line Path Generation and Tracking for High-Speed Wheeled Autonomous Vehicles

5a. CONTRACT NUMBER
W911NF-05-1-0331

5b. GRANT NUMBER

5c. PROGRAM ELEMENT NUMBER
611102

6. AUTHORS
Panagiotis Tsiotras

5d. PROJECT NUMBER

5e. TASK NUMBER

5f. WORK UNIT NUMBER

7. PERFORMING ORGANIZATION NAMES AND ADDRESSES
Georgia Tech Research Corporation
Office of Sponsored Programs
Georgia Tech Research Corporation
Atlanta, GA 30332 -0415

8. PERFORMING ORGANIZATION REPORT NUMBER

9. SPONSORING/MONITORING AGENCY NAME(S) AND ADDRESS(ES)
U.S. Army Research Office
P.O. Box 12211
Research Triangle Park, NC 27709-2211

10. SPONSOR/MONITOR'S ACRONYM(S)
ARO

11. SPONSOR/MONITOR'S REPORT NUMBER(S)
47338-NS.3

12. DISTRIBUTION AVAILIBILITY STATEMENT
Approved for public release; Distribution Unlimited

13. SUPPLEMENTARY NOTES
The views, opinions and/or findings contained in this report are those of the author(s) and should not contrued as an official Department of the Army position, policy or decision, unless so designated by other documentation.

14. ABSTRACT
TBA

15. SUBJECT TERMS
path-planning, trajectrory generation, autonomous vehicles, aggressive driving

16. SECURITY CLASSIFICATION OF:			17. LIMITATION OF ABSTRACT	15. NUMBER OF PAGES	19a. NAME OF RESPONSIBLE PERSON
a. REPORT	b. ABSTRACT	c. THIS PAGE			Panagiotis Tsiotras
U	U	U	SAR		19b. TELEPHONE NUMBER
					404-894-9526

On-Line Path Generation and Tracking for High-Speed Wheeled Autonomous Vehicles

Final Report
ARO Grant Number W911NF-05-1-0331

by

Panagiotis Tsiotras
Principal Investigator
School of Aerospace Engineering
Georgia Institute of Technology
Atlanta, GA 30332-0150

for

U.S. Army Research Office
Systems and Control
Computing and Information Science Division
P.O. Box 12211
4300 South Miami Blvd.
Research Triangle Park, NC 27709-2211

Attention
Dr. Randy Zachery
Tel: (919) 549-4368
E-mail: randy.zachery@us.army.mil

August 2009

Georgia Institute of Technology
School of Aerospace Engineering

School of Aerospace Engineering
Atlanta, Georgia 30332-0150 U.S.A.
PHONE 404-894-9526
FAX 404-894-2760

ON-LINE PATH GENERATION AND TRACKING FOR HIGH-SPEED WHEELED AUTONOMOUS VEHICLES

Final Report
ARO Grant Number W911NF-05-1-0331

Panagiotis Tsiotras
Principal Investigator
School of Aerospace Engineering
Georgia Institute of Technology
Atlanta, GA 30332-0150

Executive Summary

The main objective of this work has been to develop control algorithms capable of steering wheeled ground vehicles autonomously, by avoiding obstacles and threats, while moving in high-speed over rough/uneven terrain. It is assumed that the vehicle has only limited onboard computational resources. The ultimate objective is to build an autonomous vehicle that operates similarly to the way expert human (eg., rally race) drivers do. The emphasis on high-speed is motivated by the advantages in terms of reaction time, minimization of exposure to danger for vehicles operating in enemy territory, increase of supply line capacity and/or delivery time reduction of materiel, etc. The most noteworthy accomplishments from this research include:

- A mathematical formalization for the description and generation of aggressive maneuvers used by expert rally racing drivers (e.g., trail braking and pendulum turn) using trajectory optimization. We have thus encapsuled expert human driving knowledge which can be subsequently used in creating path and motion primitives for on-line implementation (papers [1, 2, 3, 4, 5, 6, 7, 8, 9, 10, 11, 12, 13]).
- The development of a fast multi-resolution algorithm for the on-line path generation in a partially known, changing environment. The algorithm makes use of a multi-resolution decomposition of the map that represents the environment. Obstacle boundaries are resolved with high fidelity only when (or if) the vehicle gets close to these obstacles. Far away obstacles are inconsequential for the short-term planning and hence these are approximated with lower fidelity. We therefore create a natural way of prioritizing threats and obstacles in a numerically efficient manner, without sacrificing accuracy. We can thus close the gap between strategic (decision-making) and tactical (reflexive) layers (papers [14, 15, 16, 17]).
- A kinodynamic motion-planning algorithm that blends together the path-planning and motion-planning control layers of the problem, allowing the generation of kinematically feasible trajectories directly from the geometric path planner. This is achieved by incorporating curvature information of the allowable paths via a novel modification of Dijkstra's algorithm that treats histories of cells or by creating suitable path/trajectory primitives and by combining them in such way that respects the kinodynamic constraints of the problem (papers [18, 19, 20, 21]).

The support of this award enabled one student to obtain his M.S. degree [22] (E. Bakolas), one student to complete his Ph.D. degree [23] (E. Velenis). Two more students were supported during their doctoral studies (R. Cowlagi and E. Bakolas). The doctoral thesis of E. Velenis received the Luther Long Award in Engineering Mechanics for the <u>best doctoral thesis</u> at Georgia Tech (2006). The paper "Shortest Distance Problems in Graphs Using History-Dependent Transition Costs with Application to Kinodynamic Path Planning" written by R. Cowlagi received the <u>best student paper award</u> in the 2009 American Control Conference held from June 10–12, 2009 in St. Louis, Missouri. Four (4) archival journal publications (two published and two under review) and seventeen (17) conference papers (all in peer-reviewed conferences) document the results of this work in the open literature.

Contents

List of Figures

List of Tables

1 Introduction

1.1 Motivation and Problem Statement

Study after study has shown the benefits of speed in military operations, both in terms of engaging the enemy, avoiding ambushes and successfully completing the mission. The US Army has been promoting the large-scale deployment of autonomous or semi-autonomous vehicles in the battlefield, either as part of the support supply chain (convoys) or as active participants in the battle zone. It is clear even to the non-expert that these vehicles will not survive for long in the battlefield if they are restrained to move and maneuver using the modest speeds demonstrated to date.

A class of vehicles we envision to be completely automated in the future are ground wheeled vehicles (Fig. 1(a)) that operate in hostile off-road environments (e.g., battlefields). A typical mission would be to drive the vehicle from point A to point B, avoid any obstacles, while minimizing exposure to danger; see Fig. 1(b). In general, minimization of the exposure to danger involves driving in minimum time or with maximum average velocity.

(a) (b)

Figure 1: (a) Autonomous military off-road vehicles will exhibit a high degree of tactical mobility, while eliminating the risk of loss of human lives; (b) A typical mission scenario may involve an autonomous vehicle entering a hazardous area to perform its mission objective, while avoiding obstacles and/or minimizing its exposure to enemy threats and countermeasures.

In order to increase manifold the survivability of these vehicles (thus also increasing the success rates of the mission) a new level of maneuverability is required. These vehicles will have to move in high-speed, inside a dynamically changing environment and will have to make split-second decisions with limited onboard computational resources. Our long-term research objective is to make this vision a reality.

2 Summary of Most Noteworthy Research Accomplishments

The main goal of this report is to summarize the results obtained under this research program. Since most of the technical results have appeared or will soon appear in over 21 archival journal and conference publications, below we only provide a summary of these results and remark on their significance. Further details can be found in the List of Publications at the end of this report.

2.1 Aggressive/Technical Driving for High Speed Vehicles

Following up on our previous work in this area, in [2, 4] we investigated the problem of generating near-minimum time velocity profiles for a vehicle along a specified path subject to acceleration constraints, similar to those arising from the friction ellipse between the tires of the vehicle and the ground. Initially we adopted a point mass parametrization of the vehicle. Using optimal control theory we completely solved this problem, characterizing the optimal control switching strategy in a mathematically rigorous manner. In generating the optimal velocity profile, several undesirable cases, where loss of controllability occurs, and which had been neglected in the literature, were also dealt with. A receding horizon implementation was proposed for the on-line implementation of the velocity optimizer [2, 5]. Robustness of the receding horizon algorithm is guaranteed by the use of an adaptive scheme that determines the planning and execution horizons. Figure 2 shows the application of the theory to a general case radius profile path.

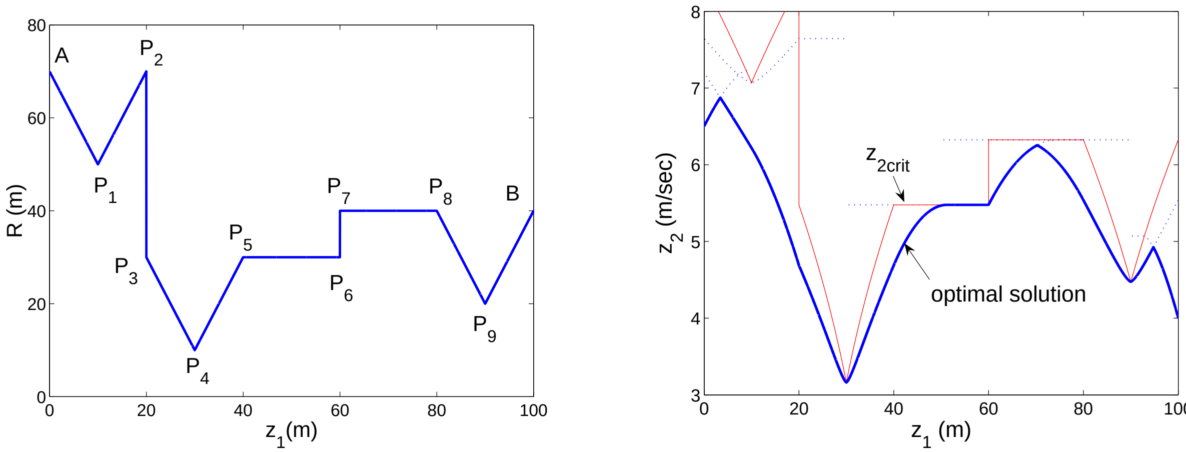

(a) (b)

Figure 2: (a) A general case radius profile path; (b) The corresponding optimal velocity profile, along with the free-boundary conditions problem solutions for constant radius and min R subarcs (from [2]).

Extensions of the point mass methodology to a half-car model are presented in [7] in order to recover the missing attitude (yaw) information. The acceleration limits (GG-diagram) of the half-car model is determined by the available tire friction forces in the front and rear axles. We have developed three extensions of the point mass methodology to the half-car model. In the first extension we directly implemented the optimal control strategy of the point mass case to the half-car model. In the second extension the optimal control strategy of the point mass case is interrupted by a stabilizing control logic when the vehicle slip angle increases beyond a certain value and the yaw dynamics tend to instability. Finally, in the third approach we enforce the additional constraint that the vehicle tracks the path with zero slip angle and determine the acceptable acceleration limits subject to the new constraint.

In [1, 9] we initiated a mathematical analysis of rally racing techniques. We provided an empirical description of Trail-Braking (TB) and Pendulum-Turn (PT) cornering, two of the most common rally racing maneuvers. We introduced a low order vehicle model that can be efficiently used within an optimization scheme. The model incorporates the appropriate level of detail to reproduce modes of operation typical of those encountered in rally, off-road racing. We have used a numerical scheme to study different trajectory optimization scenarios during cornering. We finally showed that our modeling approach is capable of reproducing TB and PT maneuvers as special cases of the minimum-time solution with additional constraints. In [8] we showed that a simple parametrization of the driver's control inputs can be used to reproduce these maneuvers using a high fidelity full-car model. Figure 3 depicts the input parameterization used for the TB maneuver. The same parameterization is valid, in fact, for a large range of corner geometries.

These numerical results were validated against experimental data (vehicles driven by professional

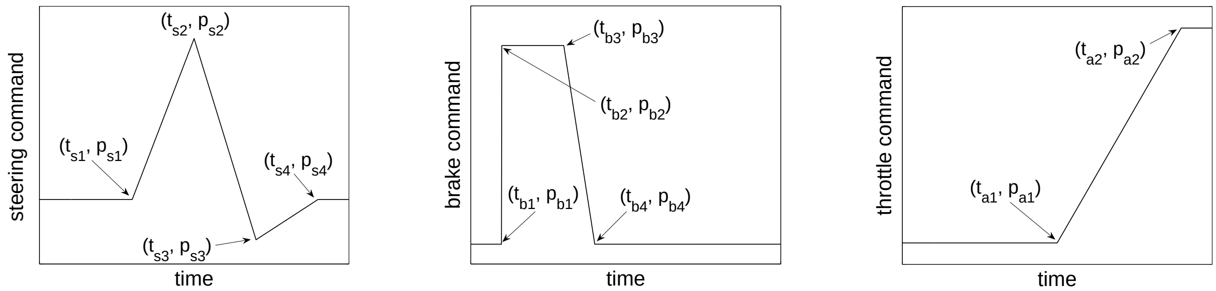

(a) (b) (c)

Figure 3: Piecewise linear parameterization for the steering, braking and throttle inputs for Trail-Braking.

rally racing drivers) collected at the facilities of Vehicle Control Center at Dalton, NH and Ford's Michigan Proving Grounds (MPG).

In [11] we relaxed the final positioning of the vehicle with respect to the width of the road in order to study the optimality of late-apex trajectories, typically followed by rally drivers. Again, it was shown that simple piecewise linear approximations of the optimal input profiles suffice to generate close to optimal TB maneuvers for a large variety of corner geometries (see Figure 4).

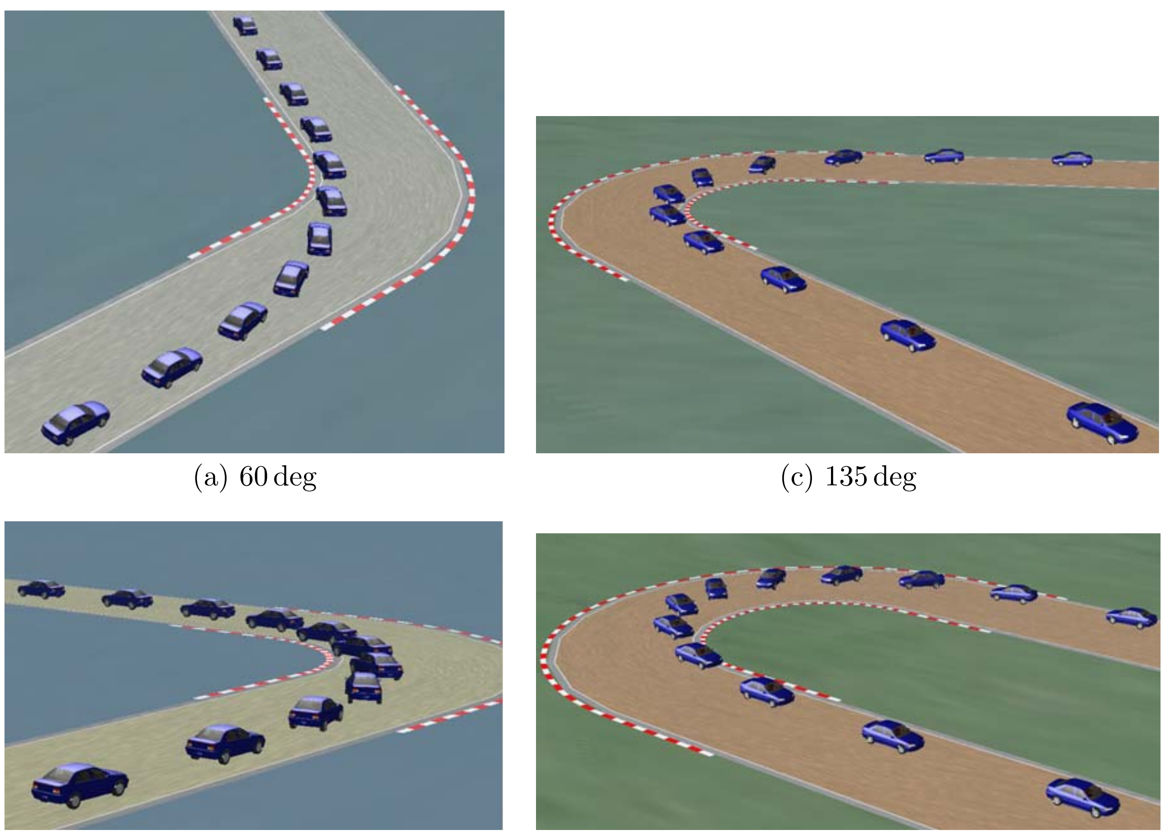

(a) 60 deg (c) 135 deg

(b) 90 deg (d) 180 deg

Figure 4: Trail-Braking through the 60, 90, 135, and 180 deg corners. Results obtained via numerical optimization. For details please refer to [1, 11].

Finally, in [3, 13] we investigated the existence and stability properties of steady-state (equilibrium) cornering conditions for a single-track vehicle model without imposing restrictive conditions on tire slip. Steady-state cornering is defined as cornering along a path of constant curvature, with constant speed and sideslip angle. The steady-state yaw rate is fixed as a function of speed and corner curvature. In contrast to traditional, neutral steering (zero vehicle slip angle), we have shown that there indeed exist multiple equilibria, many of which involve a nonzero (and often large) vehicle slip angle. This provides a mathematical justification of the sustained "drift" cornering maneuvers used by expert race/rally drivers. For each steady-state cornering condition we calculated the corresponding tire friction forces at the front and rear tires, as well as the required front steering angle and front and rear wheel slip ratios, to maintain constant velocity, turning rate and vehicle sideslip angle. We analyzed the resulting conditions, identifying stable and unstable relative equilibria. Inspired by recent progress in the understanding of advanced driving techniques, we proposed a sliding-mode control scheme stabilizing steady-state cornering conditions, using only longitudinal control inputs, i.e, accelerating/braking torques applied at the front and/or rear wheels. This is akin to the well-known "left foot braking" technique used by rally drivers to regulate the friction forces at the front and rear axles by taking advantage of the longitudinal weight transfer of the vehicle. Figure 5 shows the result from a rather extreme case of sustained cornering at a slip angle of $\beta \approx 50\,\text{deg}$.

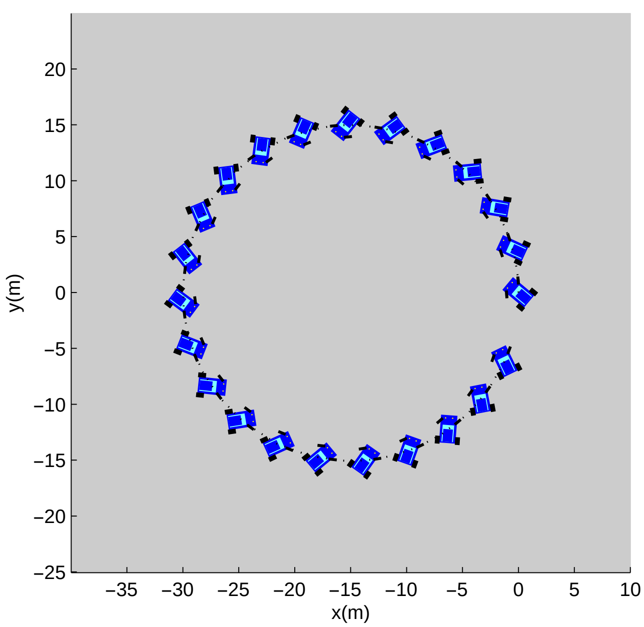

Figure 5: An example of steady-state (sustained) cornering at large vehicle slip angles. These equilibria, whose existence is shown in [13, 3], can be used to generate "on-the-fly" aggressive cornering maneuvers for autonomous vehicles.

2.2 Hierarchical Multi-resolution Path Planning

A common method for solving path planning problems based on rectangular cell approximations of the environment is to employ a graph representation. However, the dimension of the graph becomes very large as the fidelity of a global approximation of the environment increases. In fact, it has been shown in the literature that path-planning in the presence of obstacles is an NP-hard problem. In order to reduce the computational complexity of the problem, we have introduced a hybrid local/global path planning algorithm that uses district levels of fidelity (resolution) of the environment at different distances from the agent's current position. The motivation for this approach is simple: first, the agent's immediate reaction to an obstacle or a threat is needed only at the vicinity of its current position. Far away obstacles or threats do not (or should not) have a large effect of the vehicle's *immediate* motion. Therefore, the most accurate and reliable information is required at the vicinity of the vehicle. Second, the plethora of sensory information used by typical robotic vehicles (e.g., cameras, radars, laser scanners, satellite imagery) do have different ranges and resolutions. A computationally efficient path planning algorithm should be able to blend together the information provided by all these sensors and focus its computational resources on the part of the path (spatial and temporal) that needs it most. In a nutshell, a computationally efficient algorithm suitable for *on-line* implementation should be able to combine short-term tactics (reaction to unforeseen threats) with long-term strategy (planning towards the ultimate goal).

In [14, 16] we used wavelets to obtain multiresolution approximations of the configuration space at different distances from the vehicle. The wavelet transform provides a very fast decomposition[1] of the environment at different levels of resolution. The number of resolution levels, their scale, and range can all be readily adapted at each time step to yield graph representations that are commensurate to the available on-board computational resources.

Given a function $f \in \mathcal{L}^2(\mathbb{R}^2)$ we can then write its 2D wavelet decomposition as follows

$$f(x,y) \approx \sum_{k,\ell\in\mathcal{I}(J_{\min})} a_{J_{\min},k,\ell}\,\Phi_{J_{\min},k,\ell}(x,y) + \sum_{i=1}^{3}\sum_{j=J_{\min}}^{J_{\max}-1}\sum_{\substack{k\in\mathcal{K}(j)\\ \ell\in\mathcal{L}(j)}} d^i_{j,k,\ell}\Psi^i_{j,k,\ell}(x,y), \tag{1}$$

where

$$\Phi_{j,k,\ell}(x,y) = \phi_{j,k}(x)\phi_{j,\ell}(y), \qquad \Psi^i_{j,k,\ell}(x,y) = \phi_{j,k}(x)\psi_{j,\ell}(y), \quad i = 1,2,3 \tag{2}$$

with $\phi_{j,k}(x) = 2^{j/2}\phi(2^jx-k)$ and $\psi_{j,k} = 2^{j/2}\psi(2^jx-k)$ and $\phi(x)$ (scaling function) and $\psi(x)$ (mother wavelet) have compact support or they decay very fast outside a small interval so they can capture localized features of f. For the case of orthonormal wavelets the approximation coefficients are given by[2]

$$a_{j,k,\ell} = \int_{-\infty}^{\infty}\int_{-\infty}^{\infty} f(x,y)\,\Phi_{j,k,\ell}(x,y)\,\mathrm{d}x\,\mathrm{d}y \tag{3}$$

and the detail coefficients by

$$d^i_{j,k,\ell} = \int_{-\infty}^{\infty}\int_{-\infty}^{\infty} f(x,y)\,\Psi^i_{j,k,\ell}(x,y)\,\mathrm{d}x\,\mathrm{d}y. \tag{4}$$

The key property of wavelets used here is the fact that the expansion (1) induces the following decomposition of $\mathcal{L}^2(\mathbb{R}^2)$

$$\mathcal{L}^2(\mathbb{R}^2) = \mathcal{V}_J \oplus \mathcal{W}^{detail}_J \oplus \mathcal{W}^{detail}_{J+1} \oplus \cdots \tag{5}$$

where $\mathcal{V}_J = \overline{\mathrm{span}}\{\Phi_{J,k,\ell}\}_{k,\ell\in\mathbb{Z}}$ and similarly $\mathcal{W}^{detail}_j = \overline{\mathrm{span}}\{\Psi^1_{j,k,\ell}, \Psi^2_{j,k,\ell}, \Psi^3_{j,k,\ell}\}_{k,\ell\in\mathbb{Z}}$ for $j \geq J$. If we use Haar wavelets, each scaling function $\phi_{j,k}(x)$ and wavelet function $\psi_{j,k}(x)$ in the Haar system is supported on the dyadic interval $I_{j,k} = [k/2^j, (k+1)/2^j]$ of length $1/2^j$ and does not vanish in this interval. Subsequently, we may associate the functions $\Phi_{j,k,\ell}$ and $\Psi^i_{j,k,\ell}$ $(i = 1,2,3)$ with the rectangular cell $c^j_{k,\ell} = I_{j,k} \times I_{j,\ell}$.

[1]The computational complexity of the wavelet transform is of order $O(n)$ where n is the input data. This is better even than the Fast Fourier Transform which has complexity of order $O(n\log_2 n)$.

[2]In the more general case of biorthogonal wavelets projections on the space spanned by the dual wavelets and dual scaling functions should be used in (3) and (4).

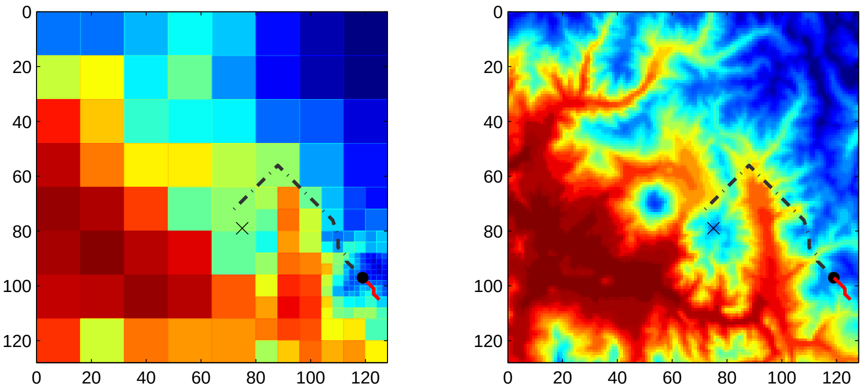

(a) $t = t_5$

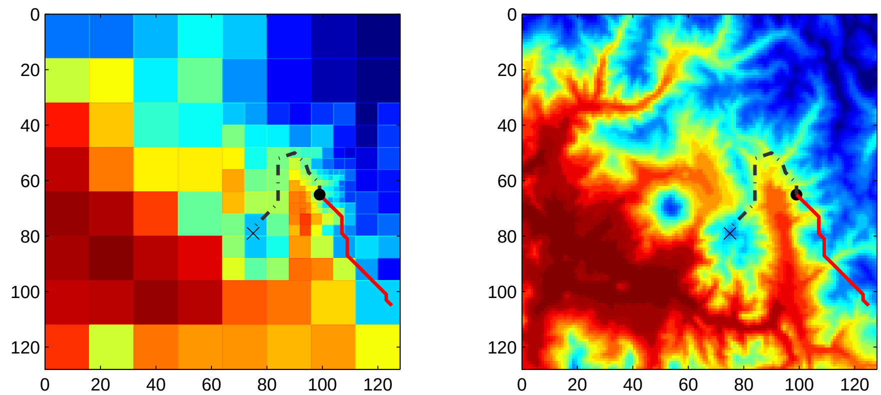

(b) $t = t_{21}$

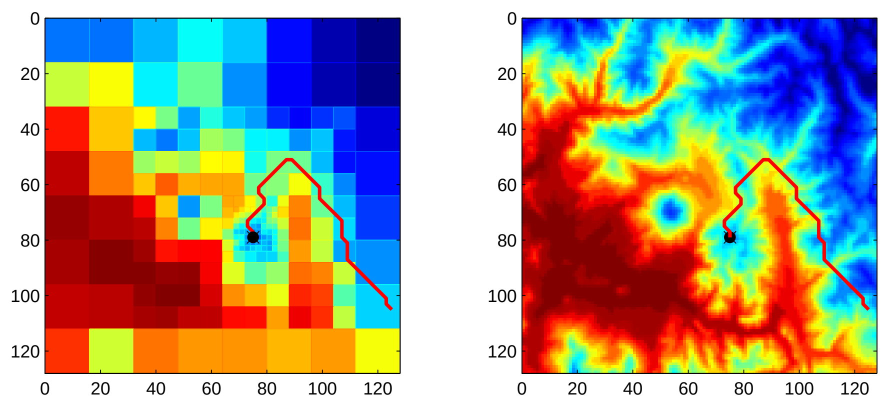

(c) $t = t_f$

Figure 6: Path evolution and replanning. Figures on the left show the multiresolution approximation of the environment with respect to the current location of the agent.

In particular, the indices of the nonzero scaling and wavelet coefficients encode the necessary information to construct the corresponding graph of the adjacency relationships of all cells. Most importantly, the dimension of this graph can be completely tailored *a priori* by choosing the minimum and maximum resolution levels $J_{\min}$ and $J_{\max}$ and the ranges (described by the allowable values of the spatial indices k and ℓ in (1) for each resolution level $J_{\min} \leq j \leq J_{\max}$. Figure 6 shows an example from the application of the algorithm to a path-planning problem using real terrain data.

Table 1: Sample results showing the computational benefits of local replanning.

	Image size (pixels)	Execution time ratio	Cost difference (%)
1.	64×64	8.46	7.17
2.	64×64	10.7	34.5
3.	64×64	9.04	16.8
3.	128×128	18.5	16.4
4.	128×128	15.4	7.95
5.	128×128	10.6	10.5
6.	256×256	51.5	2.87
7.	256×256	51.2	5.52
8.	256×256	34.1	18.8

The algorithm can also be used in case of moving obstacles and pop-up threats since replanning is performed at each step the vehicle moves to a new location. However, the algorithm performs a new cell decomposition at each iteration. Thus, it discards all information about the path other than the location of the immediately next cell. In [15] we developed a refinement of the baseline algorithm based on local replanning ideas that explores the information from the previous iteration. Table 1 shows sample comparison results between the proposed algorithm and that in [14]. It is seen that the local replanning algorithm is an order of a magnitude faster but produces paths with slightly higher costs. Also note that the savings in execution time increases with the size of the image being processed. The image sizes are in pixels, and the cost difference is the extra cost of the proposed algorithm's resultant path as a percentage of the cost of path resulting from the algorithm in [14]. The suboptimality of the path with local replanning is typically at the order of 10%. Case 2 in Table 1 is an anomalous result where the true optimal path lied mostly outside the initial sequence of cells.

Another potential problem with the baseline path-planning algorithms stems from the fact that the rectangular cell decomposition using Haar wavelets is not optimal for resolving boundaries of obstacles (see Figure 7) using onboard sensors (cameras, radars, antennas, etc) whose area of influence or field of view does not conform to the box-like topology. In fact, most typical sensor devices provide sector-like representations of the environment. In [17] we overcome this difficulty by employing a conformal mapping to map the sector cells to rectangular cells in a new coordinate system. Recall that the polar transformation maps a sector specified by the radii $\rho_{\min}$ and $\rho_{\max}$ and the angles $\theta_{\min}$ and $\theta_{\max}$ from the cartesian (x, y) plane to the polar plane thus obtaining a *rectangular* domain in the (ρ, θ) plane. Figure 8, taken from [17], demonstrates the result of this approach.

2.3 Consistent Kinodynamic Motion Planning for Autonomous Vehicles

A common approach to reduce the computational complexity of the motion-planning problem is to divide it into a geometric and a motion-planning layers. This decoupling may lead to infeasible/unrealistic paths, which cannot be executed by the vehicle. In [20] we propose a method to close this gap and use dynamic information (in the form of the maximum allowable local curvature the vehicle can negotiate) at the geometric path planning layer. Specifically, our approach modifies the well-known Dijkstra or A* algorithms to include the *history* of visited cells in the search. The idea is rather simple, although its implementation can be quite involved. Standard graph-search based algorithms look, at each step, at the transition cost between only two successive nodes (i.e., nodes). This is too restrictive in order to incorporate kinematic constraints such as maximum (local) allowable curvature. Therefore, and in order to incorporate path curvature information early on (that is, at the geometric level) while solving the motion planning problem, we work with cost functions based on $k-$tuples of nodes, for some fixed $k > 2$, such that the elements of each $k-$tuple are pairwise adjacent. The question of feasibility of traversal through $k-$tuples of cells (rather than traversal through two successive cells only) allows for more general definitions of cost functions. In particular, we can introduce transition costs that capture the maximum approximate curvature

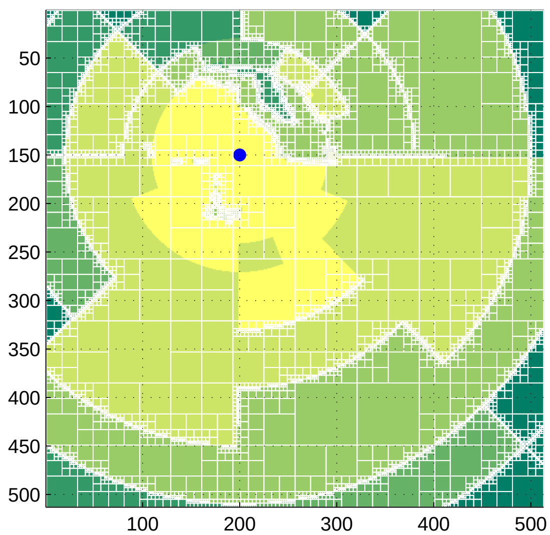

Figure 7: A cell decomposition based on the available sector approximation of the environment obtained by the on-board sensor devices of the agent (denoted with the blue dot). In order to resolve the geometry of the arc-boundary of each sector the standard quadtree algorithm generates a large number of cells close to the boundaries of these arcs.

for any path lying inside the channel. As a result, we can ensure that a feasible *trajectory* will always exist inside the computed channel of cells at the geometric, path-planning layer, even before invoking the motion-planning task.

This result is of independent, theoretical interest and can be applied to any graph-search problem. The algorithm can be used anytime a "reasonable" cost for a sequence of cells is known.

One possible instance of this idea is to associate certain sequences of cells as "good" while all others are deemed undesirable. Figure 9 shows an example of sequences of cells (i.e., tiles) inside a channel that may be assigned a good score. The algorithm penalizes the sought-after path depending on the number of good of bad sequences of tiles it contains. A much more sophisticated manner to construct good channels with the *simultaneous* construction of the corresponding path of given bounded curvature is reported in [18].

Numerical examples show that our algorithm outperforms the naive alternative of performing the search on the "lifted" graph that contains all possible combinations of sequences of cells. Table 2 shows, for several sample test cases, the ratios of the total computational times between the execution of Dijkstra's algorithm on the "lifted" graph over the execution times of the proposed algorithm.

Another approach to construct bounded curvature (and bounded curvature gradient) paths inside a *given* channel has been reported in [19, 21]. Specifically, in [19] we propose an algorithm for concatenating arcs of circles of maximum curvature and line segments (i.e., Dubins' path primitives) using a minimum look-ahead distance (just three cells). Unfortunately, direct concatenation of line segments and circle arcs will result in a discontinuity in the path curvature. Tracking such a curve will lead to poor performance. The main source of this poor performance is the latency associated to the steering command inputs of typical ground vehicles. It is therefore of interest, at least for ground wheeled vehicle applications, to consider paths which not only have a curvature bounded by a given upper bound, but also have a bound on the gradient of the curvature. In [21] we solve exactly this problem, by adding one more element in the family of path primitives: segments of clothoids.

Table 2: Comparison of execution times between the proposed algorithm and the standard Dijkstra algorithm run on the "lifted" graph.

$\|\mathcal{G}\|$	H	Avg. time ratio	$\|\mathcal{G}\|$	H	Avg. time ratio
100	1	1.1472	100	3	1.475
400	1	1.3680	225	3	1.531
1600	1	1.7551	400	3	1.536
100	2	1.8176	36	4	2.544
400	2	2.3000	64	4	2.519
900	2	3.8407	100	4	2.849

3 Collaborations and Technology Transfer

We established a close collaboration with Vehicle Control Training, LLC (POC: Greg McKinney), a company that specializes in training military and government security personnel in high-speed driving techniques, especially over rough terrain. The PI has been a leading member of the SAVE (Synthetic Automotive Virtual Environment) program, recently approved by the US congress ($1.6M for FY08 and $2.2M for FY09) for the development of high-fidelity training driving platforms for training soldiers in high speed and abnormal driving conditions. Except VCT and Georgia Tech, other members of the SAVE program team include Vehicle Control Training, MIT, US Army ERDC-Cold Regions Research & Engineering Laboratory, and SimCraft).

Realistic experimental data for validating the models describing the aggressive cornering maneuvers investigated as part of this research were collected through our established collaborations with VCT and Ford Motor Company. Ford (POC: Jianbo Lu) provided the test vehicles and allowed use of their test facilities (Michigan Proving Ground) for data collection during the summer of 2006.

Ford's interest in technical driving techniques stems from their potential application in increasing performance of current active vehicle safety systems. This has led to a collaboration with the PI's lab for the development of active safety control algorithms for commercial vehicles using these advanced driving techniques. Two provisional patents have been filled as a result of this collaboration with Ford.

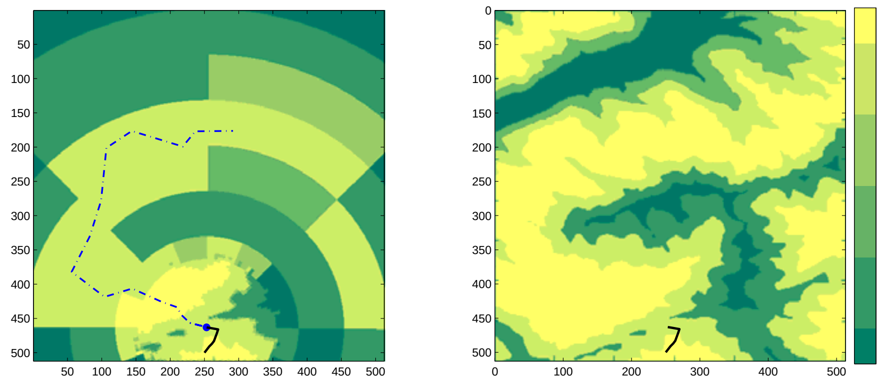

(a) $t = 4$

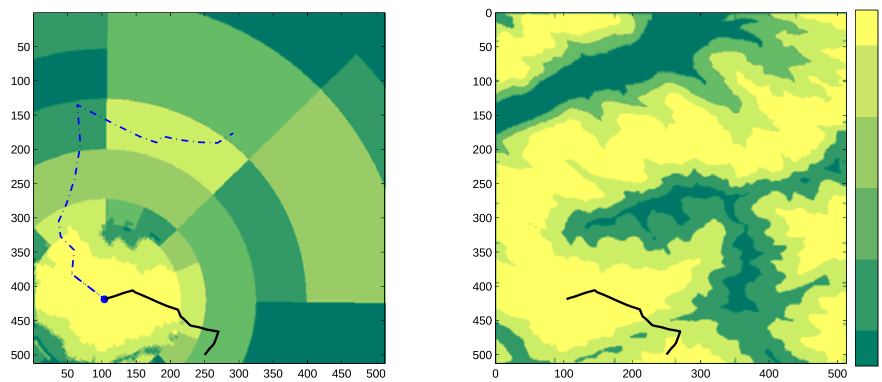

(b) $t = 10$

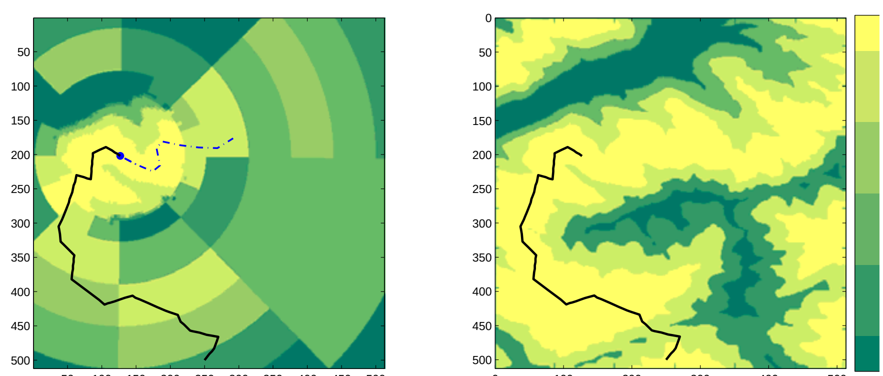

(c) $t = 22$

Figure 8: Path evolution with time. The figures show the actual path (solid line) along with the most recent tentative path (dotted line) of the agent at each time step. The agent reaches the final destination at $t = t_f$.

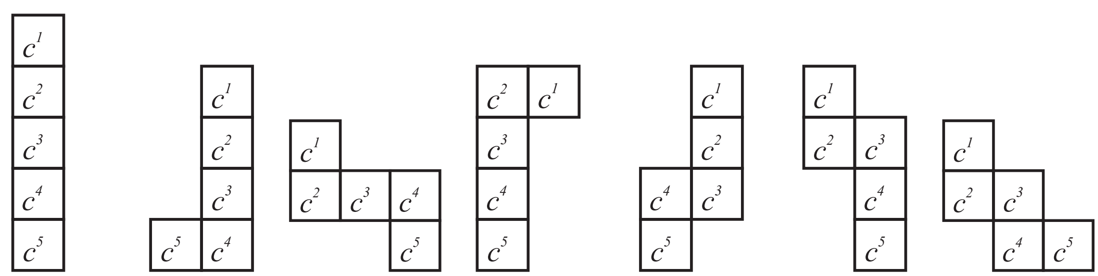

(a) $\mathcal{A}^1$ (b) $\mathcal{A}^2$ (c) $\mathcal{A}^3$ (d) $\mathcal{A}^4$ (e) $\mathcal{A}^5$ (f) $\mathcal{A}^6$ (g) $\mathcal{A}^7$

Figure 9: Illustration of tiles based on histories of three cells.

List of Publications

[1] E. Velenis, P. Tsiotras, and J. Lu, "Optimality properties and driver input parameterization for trail-braking cornering," *European Journal of Control*, vol. 14, no. 4, pp. 308–320, 2008.

[2] E. Velenis and P. Tsiotras, "Minimum-time travel for a vehicle with acceleration limits: Theoretical analysis and receding horizon implementation," *Journal of Optimization Theory and Applications*, vol. 138, no. 2, pp. 275–296, 2008.

[3] E. Velenis, E. Frazzoli, and T. P., "Steady-state cornering equilibria and stabilization for a vehicle during extreme operating conditions," *International Journal of Vehicle Autonomous Systems*, 2009. under review.

[4] E. Velenis and P. Tsiotras, "Optimal velocity profile generation for given acceleration limits: Theoretical analysis," in *Proceedings of the American Control Conference*, (Portland, OR), pp. 1478–1483, June 8 - 10 2005.

[5] E. Velenis and P. Tsiotras, "Optimal velocity profile generation for given acceleration limits: Receding horizon implementation," in *Proceedings of the American Control Conference*, (Portland, OR), pp. 2147–2152, June 8 - 10 2005.

[6] E. Velenis and P. Tsiotras, "Minimum time vs. maximum exit velocity path optimization during cornering," in *IEEE International Symposium on Industrial Electronics (ISIE05)*, (Dubrovnik, Croatia), pp. 355–360, June 20-23, 2005.

[7] E. Velenis and P. Tsiotras, "Optimal velocity profile generation for given acceleration limits: The half-car model case," in *IEEE International Symposium on Industrial Electronics (ISIE05)*, (Dubrovnik, Croatia), pp. 361–366, June 20-23, 2005.

[8] E. Velenis, P. Tsiotras, and J. Lu, "Aggressive maneuvers on loose surfaces: Data analysis and input parametrization," in *15th IEEE Mediterranean Control Conference*, (Athens, Greece), June 26–29 2007.

[9] E. Velenis, P. Tsiotras, and J. Lu, "Modeling aggressive maneuvers on loose surfaces: The cases of trail-braking and pendulum-turn," in *European Control Conference*, (Kos, Greece), pp. 1233–1240, July 2-5 2007.

[10] S. Jain, P. Tsiotras, and E. Velenis, "Optimal feedback velocity profile generation for a vehicle with given acceleration limits: A level set implementation," in *16th IEEE Mediterranean Conference on Control and Automation*, (Ajaccio, Corsica, France), pp. 451–456, June 25-26, 2008.

[11] E. Velenis, P. Tsiotras, and L. J., "Trail-braking driver input parameterization for general corner geometry," in *Motorsports Engineering Conference*, (Concord, NC), Dec. 2–4, 2008. SAE Paper 2008-01-2986.

[12] A. Scacchioli, P. Tsiotras, and J. Lu, "Nonlinear-feedback vehicle traction force control with load transfer for accident avoidance," in *ASME Dynamic Systems and Control Conference (DSCC'09)*, (Hollywood, CA), Oct. 12–14, 2009.

[13] E. Velenis, E. Frazzoli, and P. Tsiotras, "On steady-state cornering equilibria for wheeled vehicles with drift," in *48th IEEE Conference on Decision and Control*, (Shanghai, China), Dec. 16–18, 2009.

[14] P. Tsiotras and E. Bakolas, "A hierarchical on-line path-planning scheme using wavelets," in *European Control Conference*, (Kos, Greece), pp. 2806–2812, July 2–5 2007.

[15] R. Cowlagi and P. Tsiotras, "Multiresolution path planning with wavelets: A local replanning approach," in *American Control Conference*, (Seattle, WA), pp. 1220–1225, June 11-13 2008.

[16] R. Cowlagi and P. Tsiotras, "Beyond quadtrees: Cell decomposition for path planning using the wavelet transform," in *46th IEEE Conference on Decision and Control*, (New Orleans, LA), pp. 1392–1397, Dec. 12–14 2007.

[17] E. Bakolas and P. Tsiotras, "Multiresolution path planning via sector decompositions compatible to on-board sensor data," in *AIAA Guidance, Navigation, and Control Conference*, (Honolulu, HI), Aug. 18-21, 2008. AIAA Paper 2008-7238.

[18] R. Cowlagi and P. Tsiotras, "Existence and synthesis of curvature-bounded paths inside nonuniform rectangular channels," *IEEE Transactions on Robotics*, 2009. (under review).

[19] E. Bakolas and P. Tsiotras, "On-line, kinodynamic trajectory generation through rectangular channels using path and motion primitive," in *47th IEEE Conference on Decision and Control*, (Cancun, Mexico), pp. 3725–3730, Dec. 9–11, 2008.

[20] R. Cowlagi and P. Tsiotras, "Shortest distance problems in graphs using history-dependent transition costs with application to kinodynamic path planning," in *American Control Conference*, (St. Louis, MO), June 10–12, 2009. (submitted).

[21] E. Bakolas and P. Tsiotras, "On the generation of nearly optimal, planar paths of bounded curvature and curvature gradient," in *American Control Conference*, (St. Louis, MO), pp. 385–390, June 10–12, 2009.

[22] E. Bakolas, "A hierarchical on-line path planning scheme using wavelets," M.S. Thesis, School of

Aerospace Engineering, Georgia Institute of Technology, Atlanta, GA, March 2006.

[23] E. Velenis, *Analysis and Control of High-Speed Wheeled Vehicles.* Phd dissertation, Georgia Institute of Technology, School of Aerospace Engineering, May 2006.